Laser and Particle Beams (2002), *20*, 211–216. Printed in the USA.

DOI: 10.1017/S0263034602202086

New approach to dense plasma thermodynamics in the superconfiguration approximation

J.-CH. PAIN AND T. BLENSKI
CEA Saclay, DSM/DRECAM/SPAM, 91191 Gif-sur-Yvette cedex, France

(RECEIVED 14 November 2001; ACCEPTED 8 December 2001)

Abstract

We propose a new approach to the calculation of ion populations in the LTE dense plasmas in the superconfiguration approximation. The screening of plasma ions is obtained using the same free-electron chemical potential for each ion charge. This chemical potential is determined by iteration keeping the total density constant and varying the volume of each ion. In such a way our approach not only gives the charge neutrality of the plasma, but also assures that the free-electron density is equal in the vicinity of each ion. The resulting ion charge distribution is different with respect to the one obtained without imposing the constraint of equal chemical potential. For instance, the effective charge is a little bit higher, which can change the shape of the absorption spectra, especially at higher densities. Examples of absorption spectra of medium-*Z* plasmas in a temperature and density range close to the present opacity measurements are shown.

Keywords: Free-electron screening; Ionic distribution; Photoabsorption spectrum; Plasma; Superconfigurations

1. INTRODUCTION

The properties of hot dense matter are important in astrophysics and in laboratory-plasma physics. The absorption coefficients of plasmas in local thermodynamic equilibrium (LTE) play an important role in radiative transfer in inertial fusion, as well as in stellar atmospheres. In the theoretical calculations in atomic physics of dense plasmas, it is necessary to have a proper treatment of the plasma thermodynamics and of the free-electron screening in the plasma. The present work improves our previous approach to the plasma thermodynamics in the superconfiguration approximation. The main idea is that all ions should have the same free electronic environment in the plasma. For that reason, the free-electron density should be equal at the boundary of each ion. Here we present an approach that allows us to assure that equality in our model.

Comparisons between ionic distributions, effective charges, and photoabsorption spectra from the previous and new methods will be shown and discussed.

Address correspondence and reprint requests to: Jean-Christophe Pain, CEA Saclay, DSM/SPAM, 91191 Gif-sur-Yvette cedex, France. E-mail: pain@drecam.saclay.cea.fr

2. THE SUPERCONFIGURATION METHOD

2.1. Definitions and method

The superconfiguration (SC) approximation has been introduced by Bar Shalom *et al.* (1989) in their superconfiguration transition arrays (STA) method of photoabsorption calculation. An SC is made of supershells that are groups of shells close in energy. For example $\Xi_1 = (1s2s2p3s)^{10}(3p3d)^6(4s4p4d\ldots)^1$ and $\Xi_2 = (1s2s2p3s)^{10}(3p)^5(3d)^1(4s4p4d\ldots)^1$ are two superconfigurations that consist, respectively, in three and four supershells. One can notice that Ξ_1 contains more configurations than Ξ_2 because $(3p3d)^6 = (3p)^6(3d)^0 \cup (3p)^5(3d)^1 \cup (3p)^4(3d)^2 \cup \ldots$.

The SC approximation has many advantages: an SC can include a large number of configurations and even all of them. It has integer shell occupation numbers, which allows one to take into account correctly the exchange terms. The method is iterative and one can always divide supershells until the spectrum converges.

Our standard approach to superconfigurations has been described elsewhere (Blenski *et al.*, 1997, 2000). The method starts with an average atom (AA) calculation, which gives,

for a given temperature and density, an average configuration with fractional shell occupation numbers and an average charge of the ions in the plasma. On the basis of these results, the supershells are defined (automatically or manually) and a set of superconfigurations is prepared by redistribution of bound electrons on the supershells. Using the AA eigen-energies and wavefunctions, the code determines preliminary probabilities of the proposed superconfigurations and retains the most probable. Then starts the self-consistent-field (SCF) calculation for each SC. The SCF equations are obtained from the minimization of the free-energy of the SC with the imposed constraints of the supershell occupation numbers. As in the AA model, we use for each SC the free-electron screening inside the Wigner–Seitz sphere using the Thomas–Fermi free-electron density. From the SCF calculation, we get for each SC the one-electron basis, which allows us to calculate the relevant many-electron quantities. The quality of that one-electron basis which is calculated self-consistently for each SC, allows one to obtain realistic optical spectra from the SC method. The calculation of photoabsorption spectra for each superconfiguration uses the Hartree–Fock energy formulas, the unresolved transition arrays (UTA) or spin orbit split arrays (SOSA) term formulas (Bauche-Arnoult *et al.*, 1979, 1982*a*, 1982*b*) which enter the statistical sums (partition functions) in order to evaluate three moments characterizing each electron-hole transition (Bar Shalom *et al.*, 1989; Blenski *et al.*, 1997, 2000).

Each SC having an integer number of bound electrons, the SCs of the same charge can be grouped into "ions" and one can calculate different average quantities for each ion, as the average free-electron chemical potential of the ion. The latter quantity depends mainly on the SC's ion charge.

2.2. New thermodynamics

In our standard approach (Blenski *et al.*, 2000), each SC has a different free-electron chemical potential μ_f, depending mainly on the charge of the SC and to some extent on its SCF potential. Therefore beyond the Wigner–Seitz sphere, each SC has, in principle, a different value of the free-electron density. Such description does not take into account the fact that all ions are in the same free-electron bath. That is why in the new method presented here, the screening of plasma ions is obtained by requiring the same free-electron chemical potential for each ion charge. In the calculation presented in this article, we use the local-density version of the SCO code presented in Blenski *et al.* (1997).

3. BASIC EQUATIONS

Initially all SCs are calculated using the same density, which is the total density of the plasma ρ_{tot}. The SCs are then grouped into "ions" and the average chemical potential is calculated for each ion. In our new approach we allow the ions to have different partial densities.

Let I be the total number of ion charges. The equality of all free-electron chemical potentials requires $(I-1)$ nonlinear equations. For each $k \in [1, I-1]$, one has

$$\mu_k(\rho_k) = \mu_{k+1}(\rho_{k+1}), \tag{1}$$

where μ_k and ρ_k represent, respectively, the free-electron chemical potential and the density of ions of charge Z_k. The dependence of μ_k on the density ρ_k is highly nonlinear and nonexplicit since it is obtained from the SCF calculation.

One has to assure the preservation of total density (or total volume)

$$\sum_{k=1}^{I} \frac{p_k}{\rho_k} = \frac{1}{\rho_{tot}}, \tag{2}$$

where p_k represents the fraction of charge state Z_k.

It is useful to write the system of equations in the following vector form:

$$\mathbf{F}(\boldsymbol{\rho}) = \begin{pmatrix} F_1(\boldsymbol{\rho}) \\ F_2(\boldsymbol{\rho}) \\ F_3(\boldsymbol{\rho}) \\ \cdot \\ \cdot \\ \cdot \\ F_{I-1}(\boldsymbol{\rho}) \\ F_I(\boldsymbol{\rho}) \end{pmatrix} = \begin{pmatrix} \mu_1(\rho_1) - \mu_2(\rho_2) \\ \mu_2(\rho_2) - \mu_3(\rho_3) \\ \mu_3(\rho_3) - \mu_4(\rho_4) \\ \cdot \\ \cdot \\ \cdot \\ \mu_{I-1}(\rho_{I-1}) - \mu_I(\rho_I) \\ \sum_{k=1}^{I} \frac{p_k}{\rho_k} - \frac{1}{\rho_{tot}} \end{pmatrix} = \mathbf{0}, \tag{3}$$

where

$$\boldsymbol{\rho} = \begin{pmatrix} \rho_1 \\ \rho_2 \\ \cdot \\ \cdot \\ \cdot \\ \rho_I \end{pmatrix}$$

is the ion-densities vector.

Once the solution vector $\boldsymbol{\rho}$ is obtained, the corresponding ionic fractions ($p_k, k \in [1, I]$) are given by the SCF code. To solve this system, we use the multidimensional Newton method. A Taylor development of vector-function $\mathbf{F}$ gives

$$\mathbf{F}(\boldsymbol{\rho}^{(i+1)}) = \mathbf{F}(\boldsymbol{\rho}^{(i)}) + (\boldsymbol{\rho}^{(i+1)} - \boldsymbol{\rho}^{(i)}) \cdot \frac{\partial \mathbf{F}}{\partial \boldsymbol{\rho}}\bigg|_{\boldsymbol{\rho}^{(i)}}. \tag{4}$$

We put

$$\mathbf{F}(\boldsymbol{\rho}^{(i+1)}) = 0, \tag{5}$$

https://doi.org/10.1017/S0263034602202086 Published online by Cambridge University Press

which means that the development can be written

$$\boldsymbol{\rho}^{(i+1)} = \boldsymbol{\rho}^{(i)} + \delta\boldsymbol{\rho}^{(i)} \tag{6}$$

where i is the iteration number and

$$\delta\boldsymbol{\rho}^{(i)} = -(J)^{-1}\cdot\mathbf{F}(\boldsymbol{\rho}^{(i)}). \tag{7}$$

(J) is the following matrix:

$$(J) = \begin{pmatrix} \frac{\partial F_1}{\partial \rho_1} & \frac{\partial F_1}{\partial \rho_2} & 0 & . & . & . & 0 \\ 0 & \frac{\partial F_2}{\partial \rho_2} & \frac{\partial F_2}{\partial \rho_3} & 0 & . & . & . \\ 0 & 0 & . & . & . & . & . \\ . & . & . & . & . & . & . \\ . & . & . & . & . & . & 0 \\ 0 & . & . & . & 0 & \frac{\partial F_{I-1}}{\partial \rho_{I-1}} & \frac{\partial F_{I-1}}{\partial \rho_I} \\ \frac{\partial F_I}{\partial \rho_1} & \frac{\partial F_1}{\partial \rho_2} & . & . & . & \frac{\partial F_I}{\partial \rho_{I-1}} & \frac{\partial F_I}{\partial \rho_I} \end{pmatrix}. \tag{8}$$

In this matrix, only diagonal, over-diagonal, and last-line terms are nonzero. For this reason it is easy to invert analytically. Once the solution vector is obtained, the corresponding ionic fractions (p_k, $k \in [1, I]$) can be calculated from the SC code. It is interesting to study the ionic distribution and to calculate the effective (average) charge of the plasma given by our method. We present below some results on nickel plasmas. We chose nickel ($Z = 28$) because many experiments have been performed on nickel plasmas (Chenais-Popovics *et al.*, 2001, in press). Nickel is close to iron ($Z = 26$), and thin nickel foils are easier to fabricate than iron foils since it is chemically less reactive. Iron, nickel, and other metals can dominate the radiative properties in the sun's interior and the knowledge of the absorption coefficients in different plasma conditions can help us to understand the interior of the sun. The interpretation of helioseismologic data is highly dependent on the iron opacity data introduced in the astrophysical models (Turck-Chièze *et al.*, 1997).

4. RESULTS AND DISCUSSION

4.1. Changes of the effective charge and the charge distribution

4.1.1. Constant density and variable temperature

At constant density, the effective charge Z^* obtained with the new method is systematically higher than the one obtained with the previous method. For $T \leq 100$ eV approximately, one can notice that ΔZ^* increases significantly and for higher temperatures it remains globally constant. The effect becomes more important for higher densities (Tables 1, 2, and 3; Fig. 1).

Table 1. *Evolution of Z^* (effective charge of the plasma) and $\Delta Z^* = Z^*(\text{New method}) - Z^*(\text{Old method})$ for density = 0.004 g/cm^3 and different values of temperature for nickel. Three effective charges are given: the one given by the average atom calculation, the one given by the previous superconfiguration method, and the one given by the superconfiguration method with the new thermodynamics*

	Z^*			
Temperature	Average atom	Old method	New method	ΔZ^*
16 eV	5.68	5.76	6.30	0.54
20 eV	6.69	6.73	7.33	0.60
24 eV	7.64	7.64	8.30	0.66
25 eV	7.87	7.87	8.54	0.67
35 eV	10.05	10.05	10.86	0.81
50 eV	12.86	12.90	13.85	0.95
100 eV	17.50	17.53	17.83	0.30
125 eV	18.21	17.84	17.94	0.10
150 eV	19.38	19.29	20.02	0.73

4.1.2. Constant temperature and variable density

At constant temperature, ΔZ^* is an increasing function of density over a wide range of densities and the charge difference ΔZ^* can take significant values (about 1 charge unit and even more; Tables 4 and 5; Fig. 2). This effect appears to be mostly a "density effect."

Table 2. *Evolution of Z^* (effective charge of the plasma) and $\Delta Z^* = Z^*(\text{New method}) - Z^*(\text{Old method})$ for density = 0.1 g/cm^3 and different values of temperature for nickel. Three effective charges are given: the one given by the average atom calculation, the one given by the previous superconfiguration method, and the one given by the superconfiguration method with the new thermodynamics.*

	Z^*			
Temperature	Average atom	Old method	New method	ΔZ^*
5	1.72	1.84	2.08	0.24
25	5.89	5.91	6.68	0.77
50	9.58	9.67	10.83	1.16
75	12.45	12.56	13.85	1.29
100	14.60	14.68	15.96	1.28
125	15.91	15.99	16.98	1.01
150	16.85	16.87	17.78	0.91
175	17.82	17.75	18.79	1.04
185	18.23	18.15	19.24	1.09
205	19.07	18.98	20.17	1.19
215	19.48	19.41	20.62	1.21

https://doi.org/10.1017/S0263034602202086 Published online by Cambridge University Press

Table 3. *Evolution of Z^* (effective charge of the plasma) and $\Delta Z^* = Z^*(New\ method) - Z^*(Old\ method)$ for density = 1.0 g/cm^3 and different values of temperature for nickel. Three effective charges are given: the one given by the average atom calculation, the one given by the previous superconfiguration method, and the one given by the superconfiguration method with the new thermodynamics*

	Z^*			
Temperature	Average atom	Old method	New method	ΔZ^*
25 eV	5.33	5.11	5.72	0.61
50 eV	7.84	8.06	9.12	1.06
100 eV	12.17	12.27	13.74	1.47
150 eV	14.67	14.68	16.07	1.39
205 eV	16.57	16.54	17.93	1.39
215 eV	16.92	16.96	18.28	1.39
225 eV	17.27	17.20	18.64	1.44
235 eV	17.62	17.53	19.00	1.47

Table 4. *Evolution of Z^* (effective charge of the plasma) and $\Delta Z^* = Z^*(New\ method) - Z^*(Old\ method)$ for T = 100 eV and different values of density for nickel. Three effective charges are given: the one given by the average atom calculation, the one given by the previous superconfiguration method, and the one given by the superconfiguration method with the new thermodynamics*

	Z^*			
Density	Average atom	Old method	New method	ΔZ^*
0.004 g/cm^3	17.50	17.53	17.83	0.30
0.01 g/cm^3	16.99	17.04	17.56	0.52
0.1 g/cm^3	14.60	14.68	15.97	1.29
1.0 g/cm^3	12.17	12.27	13.74	1.47

4.2. Photoabsorption spectra

The new approach has been implemented in the superconfiguration code SCO (Blenski *et al.*, 1997, 2000) which calculates the photoabsorption spectra. In the new version of the code, a spectrum is now calculated separately for each ion using the obtained ionic density and the total spectrum is found as the sum of partial spectra taking into account the abundance of each ion.

In the case of a nickel plasma at $T = 20$ eV and at density = 0.004 g/cm^3, one can see that the differences between the spectra obtained with the new and old methods are not very important (Fig. 3). But at higher density and temperature (see, e.g., the case of $T = 100$ eV and density = 0.01 g/cm^3; Fig. 4), one can notice quite important differences in the bound–bound absorption structures and also in the bound–free part of the spectrum (photoelectric effect). The bound–free photoabsorption calculated with the new method is nearly twice as large as the photoabsorption calculated with the previous one.

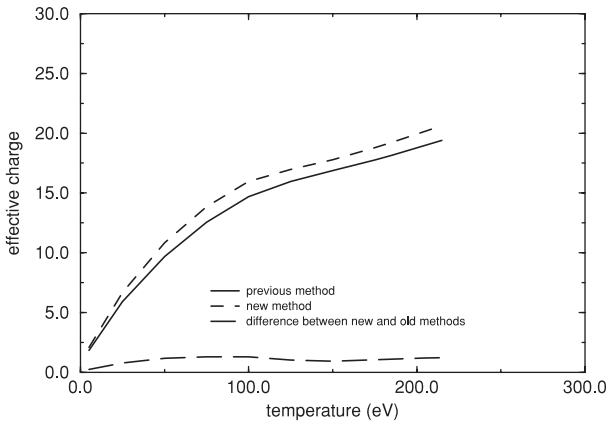

Fig. 1. Evolution of effective charge versus temperature for density = 0.1 g/cm^3.

5. CONCLUSION

The proposed method converges very fast (only a few iterations are needed). It assures that the plasma is electrically neutral, and that the free-electron density is equal at the boundary of each ion. In these conditions, the resulting ion charge distribution is different with respect to the one obtained without imposing the constraint of equal chemical potential for each ion. The effective charge Z^* is always higher, and this difference can take significant values. This implies that the shape of photoabsorption spectra is different (especially at high plasma densities, where the "correlations" between ions via the free-electron bath become important).

We are now looking at the influence of the atomic number Z on the effective charge and on the charge distribution. It

Table 5. *Evolution of Z^* (effective charge of the plasma) and $\Delta Z^* = Z^*(New\ method) - Z^*(Old\ method)$ for T = 150 eV and different values of density for nickel. Three effective charges are given: the one given by the average atom calculation, the one given by the previous superconfiguration method, and the one given by the superconfiguration method with the new thermodynamics*

	Z^*			
Density	Average atom	Old method	New method	ΔZ^*
0.004 g/cm^3	19.38	19.29	20.02	0.73
0.01 g/cm^3	18.76	18.67	19.36	0.69
0.1 g/cm^3	16.85	16.87	17.78	0.91
1.0 g/cm^3	14.67	14.68	16.07	1.39

https://doi.org/10.1017/S0263034602202086 Published online by Cambridge University Press

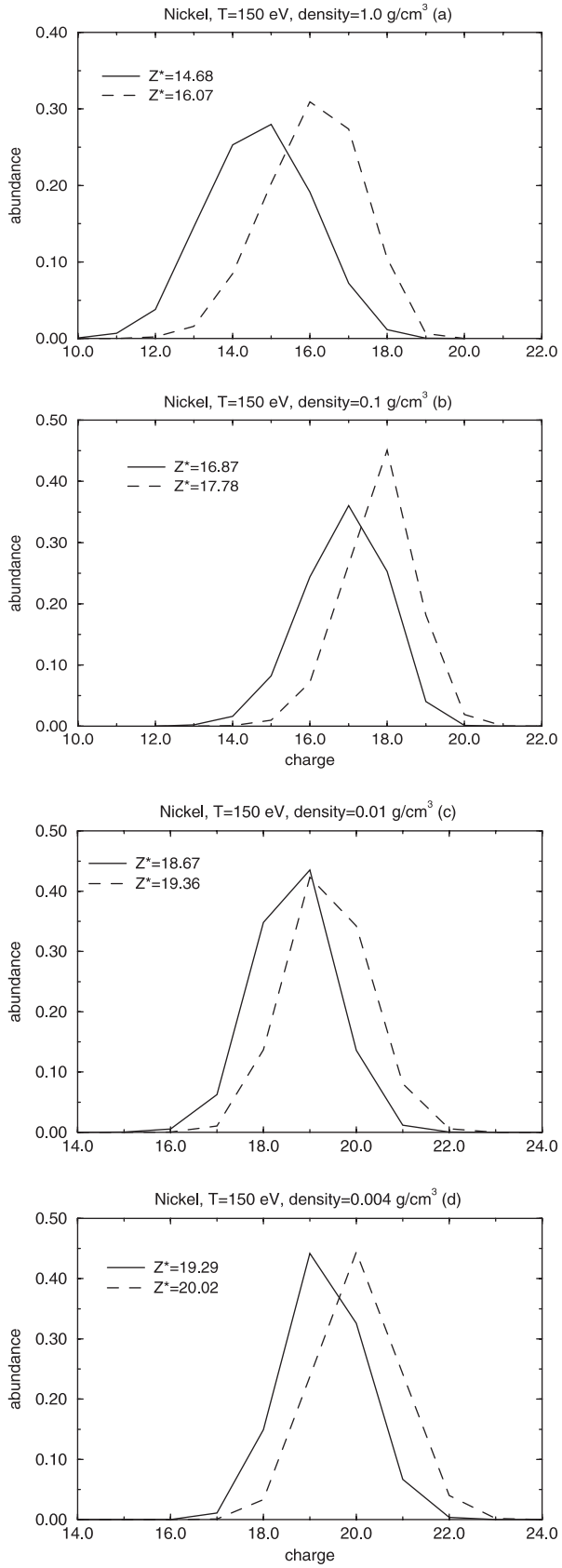

Fig. 2. Ionic distributions for $T = 150$ eV and different values of density: 1.0 g/cm^3 (a), 0.1 g/cm^3 (b), 0.01 g/cm^3 (c), and 0.004 g/cm^3 (d) with previous (solid line) and new (dashed line) methods.

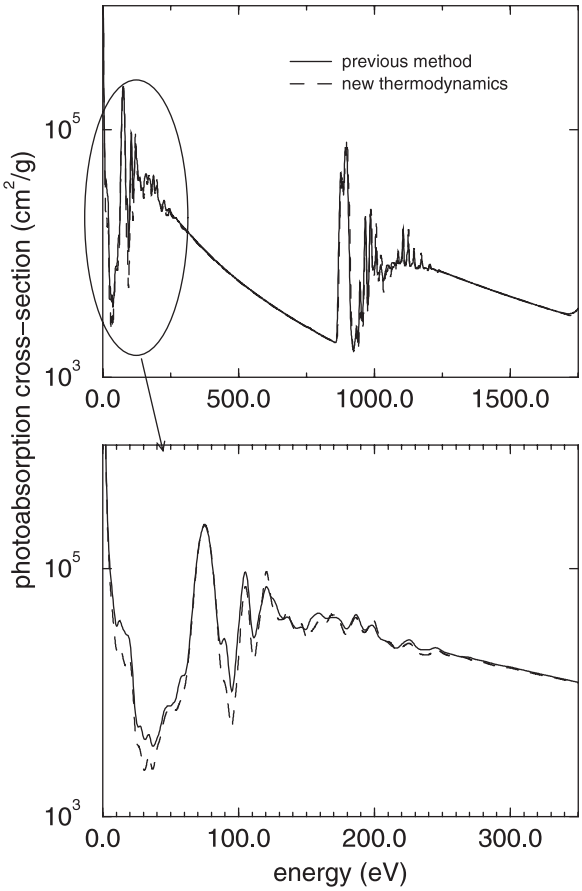

Fig. 3. Photoabsorption spectrum for nickel with $T = 20$ eV and density = 0.004 g/cm^3.

can be important for Al/Ni multilayer experiments (Chenais-Popovics *et al.*, 2001) for example, where Al is used as a thermometer (the contributions of the different ions to the photoabsorption are well separated; Fig. 5).

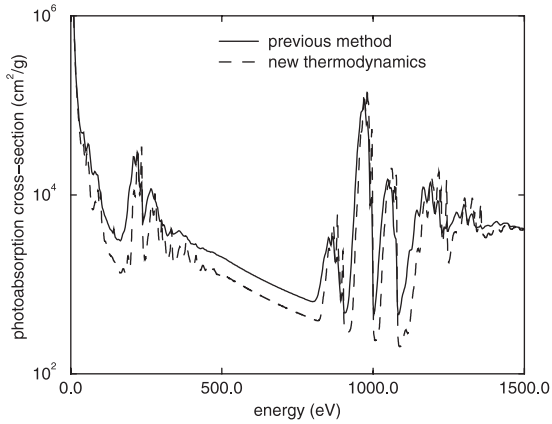

Fig. 4. Photoabsorption spectrum for nickel with $T = 100$ eV and density = 0.01 g/cm.

https://doi.org/10.1017/S0263034602202086 Published online by Cambridge University Press

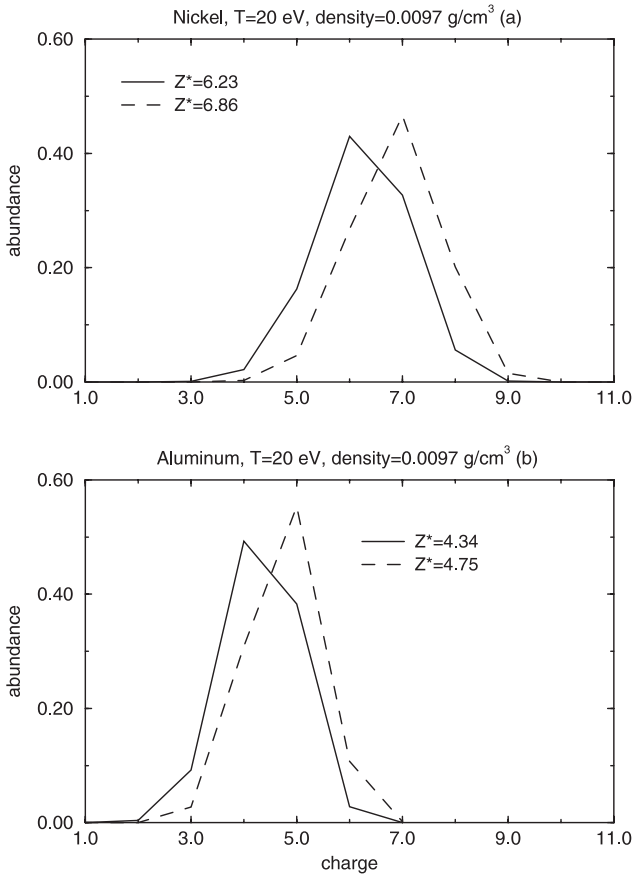

Fig. 5. Ionic distributions of previous and new methods for nickel (a) and aluminum (b) with $T = 20$ eV and density $= 0.0097$ g/cm^3 with previous (solid line) and new (dashed line) methods.

More comparisons with recent experiments and with future-generation-laser experiments still have to be done. The ultimate goal of this work is the extension of the method to mixtures of different elements, for example for Al/Ni plasmas (Chenais-Popovics *et al.*, 2001), or the interior of the sun.

NOTE ADDED IN PROOF

We have recently found that one should impose at the equilibrium the equality of pressure at the ion boundary instead of the equality of the chemical potential. This result, together with the inclusion of the work term into the ion free energy may lead to considerably different distributions of ionic probabilities. The work on that new approach is in progress.

REFERENCES

Bar Shalom, A. Oreg, J., Goldstein, W.H. Shvarts, D. & Zigler, A. (1989). *Phys. Rev. A* **40**(6), 3183–3193.

Bauche Arnoult, C., Bauche, J. & Klapisch, M. (1979). *Phys. Rev. A* **20**(6), 2424–2439.

Bauche Arnoult, C., Bauche, J. & Klapisch, M. (1982*a*). *Phys. Rev. A* **25**(5), 2641–2646.

Bauche Arnoult, C., Bauche, J. & Klapisch, M. (1982*b*). *Phys. Rev. A* **31**(4), 2248–2259.

Blenski, T., Grimaldi, A. & Perrot, F. (1997). *Phys. Rev. E* **55**, R4889–R4892.

Blenski, T., Grimaldi, A. & Perrot, F. (2000). *J. Quant. Spectrosc. Radiat. Transfer* **65**, 91–100.

Chenais-Popovics, C., Gilleron, F., Fajardo, M., Merdji, H., Miβalla, T., Gauthier, J.C., Renaudin, P., Gary, S., Bruneau, J., Perrot, F., Blenski, T., Fölsner, W. & Eidmann, K. (2001*a*). *J. Quant. Spectrosc. Radiat. Transfer* **65**, 117–133.

Chenais-Popovics, C., Fajardo, M., Gauthier, J.C., Thais, F., Gilleron, F., Pain, J.C., Blenski, T., Fölsner, W. & Eidmann, K. (2001*b*). Presented at the IFSA 2001 Conference, Kyoto, September 9–14, 2001.

Chenais-Popovics, C., Fajardo, M., Gilleron, F., Teubner, U., Gauthier, J.C., Bauche Arnoult, C., Bachelier, A., Bauche, J., Blenski, T., Thais, F., Perrot, F., Benuzzi, A., Turck, Chièze, S., Chièze, J.P., Dorchies, F., Andiel, U., Fölsner, W. & Eidmann, K. (2002). *Phys. Rev. E* **65**, 016413–016422.

Pain, J.C. & Blenski, T., to be published.

Turck-Chièze, S., Basu, S., Brun, A.S., Christensen-Dalsgaard, J., Eff-Dawich, A., Lopes, I., Pérez-Hernandez, F., Berthomieu, G., Provost, J., Ulrich, R.K., Baudin, F., Boumier, P., Charra, J., Gabriel, A.H., Garcia, R.A., Grec, G., Renaud, C., Robillot, J.M., Roca Cortès, T. (1997). *Sol. Phys.* **175**, 247.

https://doi.org/10.1017/S0263034602202086 Published online by Cambridge University Press